Journal of Advanced Research (2016) 7, 143–154

Cairo University

Journal of Advanced Research

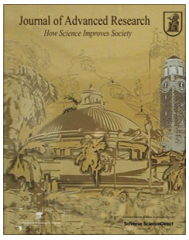

ORIGINAL ARTICLE

Efficiency of calcium phosphate composite nanoparticles in targeting Ehrlich carcinoma cells transplanted in mice

Eman I. Abdel-Gawad [a], **Amal I. Hassan** [a,*], **Sameh A. Awwad** [b]

[a] *Radioisotopes Department, Atomic Energy Authority, Egypt*
[b] *Egyptian Army Forces, Egypt*

ARTICLE INFO

Article history:
Received 7 November 2014
Received in revised form 29 March 2015
Accepted 3 April 2015
Available online 22 April 2015

Keywords:
Nanomedicine
Calcium phosphate (CaP) nanoparticles
EAC transplantation
Solid tumor
Neurotransmitters

ABSTRACT

The present study aimed to investigate the mode of action of nano-CaPs *in vivo* as a therapy for solid tumor in mice. To achieve this goal, Ehrlich Ascites Carcinoma (EAC) was transplanted into 85 Swiss male albino mice. After nine days, the mice were divided into 9 groups. Groups 1 and 2 were allocated as the EAC control. Groups 3 and 4 were injected once intratumorally (IT) by nano-calcium phosphate (nano-CaP). Groups 5 and 6 received once intraperitoneal injection (IP) of nano-CaP. Groups 7, 8, and 9 received nano-CaP (IP) weekly. Blood samples and thigh skeletal muscle were collected after three weeks from groups 1, 3, 5, and 7 and after four weeks from groups 2, 4, 6, and 8. On the other hand, group 9 received nano-CaP (IP) for four weeks and lasted for three months to follow up the recurrence of tumor and to ensure the safety of muscle by histopathological analysis. Tumor growth was monitored twice a week throughout the experiment. DNA fragmentation of tumor cells was evaluated. In thigh tissue, noradrenaline, dopamine, serotonin (5HT), and gamma-aminobutyric acid (GABA) were measured. In serum, 8-Hydroxy-deoxyguanosine (8-OHDG), adenosine triphosphate (ATP), and vascular endothelial growth factor (VEGF) were analyzed. Histopathological and biochemical results showed a significant therapeutic effect of nano-CaP on implanted solid tumor and this effect

Abbreviations: EAC, Ehrlich Ascites Carcinoma; Nano-CaP, nano calcium phosphate; GABA, gamma aminobutyric acid; 5HT, serotonin; 8-OHDG, 8-hydroxy-deoxyguanosine; ATP, adenosine triphosphate; IP, intraperitoneal; IT, intratumoral; FAK, focal adhesion kinase; DNA, deoxyribonucleic acid; MAPK, mitogen-activated protein kinase; XRD, X-ray diffraction; FTIR, Fourier transform infrared; SEM, scanning electron microscopy; TEM, transmission electron microscope; RIR, reference intensity ratio; VEGFR2, vascular endothelial growth factor receptor 2.

* Corresponding author. Tel.: +20 1112900054.
E-mail address: virtualaml@gmail.com (A.I. Hassan).

Peer review under responsibility of Cairo University.

Production and hosting by Elsevier

http://dx.doi.org/10.1016/j.jare.2015.04.001

was more pronounced in the animals treated IP for four weeks. This improvement was evident from the repair of fragmented DNA, the significant decrease of caspase-3, 8-OHDG, myosin, and VEGF, and the significant increase of neurotransmitters (NA, DA, 5HT, and GABA). Additionally, histopathological examination showed complete recovery of cancer cells in the thigh muscle after three months.

Introduction

Cancer nanotechnology provides a unique approach and comprehensive technology against cancer through early diagnosis, prediction, prevention, and personalized therapy and medicine [1]. Nanoparticles provide opportunities for designing and tuning properties that are not possible with other types of therapeutic drugs due to its ability to interact with cells and tissues at a molecular level which provides them with a distinct advantage over other polymeric or macromolecular substances [2]. As with any cancer therapy, the key issue is to achieve the desired concentration of therapeutic agent in tumor sites, thereby destroying cancerous cells while minimizing damage to normal cells [3]. Frequent challenges encountered by current cancer therapies include nonspecific systemic distribution of antitumor agents, inadequate drug concentrations reaching the tumor site, intolerable cytotoxicity, limited ability to monitor therapeutic responses, and development of multiple drug resistance [4]. In addition to the complex physiological and biochemical factors tumoral processes involve, and numerous observations concluded that tumor cells, as biological entities, interact with their surrounding cells, lymphatic circulation, blood circulation and nervous system [5]. Thus, the use of biocompatible materials of biological origin is paramount for biomedical applications in supports, casings, or implants needed to integrate within the human body to minimize immune responses. Among them, calcium phosphate particles had a suppressive effect on the proliferation of tumor cells. Since it was almost impossible to excise malignant tumor completely due to their capability of rapid proliferation, local invasion and distance migration, the influence of the nanoparticles of calcium phosphate with different morphology, size, and ions substitution on tumor cells, especially highly malignant ones, was significant in clinic [6]. The granular morphologies of the CaP nanoparticles (i.e., isotropic structure) are also likely to affect their biological effects [7]. So, these particles inhibit the proliferation of tumor cells and do not cause the threat for health.

Based on the effects of administration route, particle size and properties on biodistribution, a variety of nanoparticulate designs have been proposed for cancer therapy and diagnosis. Targeting of tumor tissues occurs through the extravasation of nanoparticles post-injection into the systemic blood circulation. The biodistribution of these particles is dependent on the characteristics of blood capillaries in the organs and tissues as well as the administration site, particle size and surface properties [8]. Even in intratumoral (i.t.) administration, understanding the mechanism of the extravasation is critical to retain the particles at the injection sites. In addition to such macro biodistribution of particles, their diffusion in the tissues, association to cells, internalization into the cells and intracellular distribution are important issues in cancer therapy and diagnosis [9]. Moreover, recent study has investigated the potential of calcium phosphate nanoparticles for transcutaneous vaccine delivery [10] and can be used also as multifunctional tools for near-infrared fluorescence (NIRF) optical imaging and Photodynamic therapy (PDT) [11]. The current study aimed to investigate the ability of nano-calcium

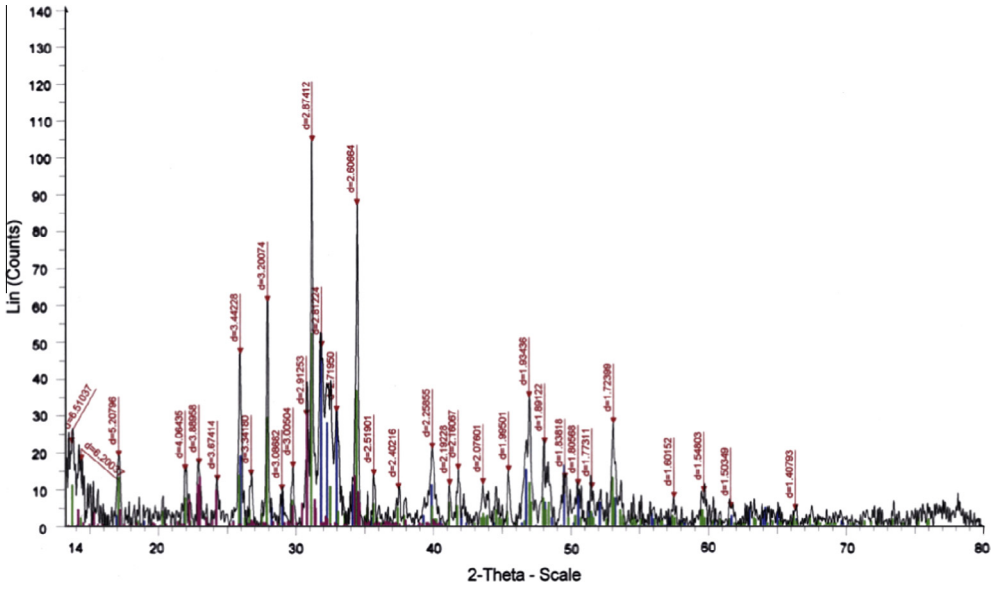

Fig. 1 XRD patterns of the sample prepared calcined at 1000 °C.

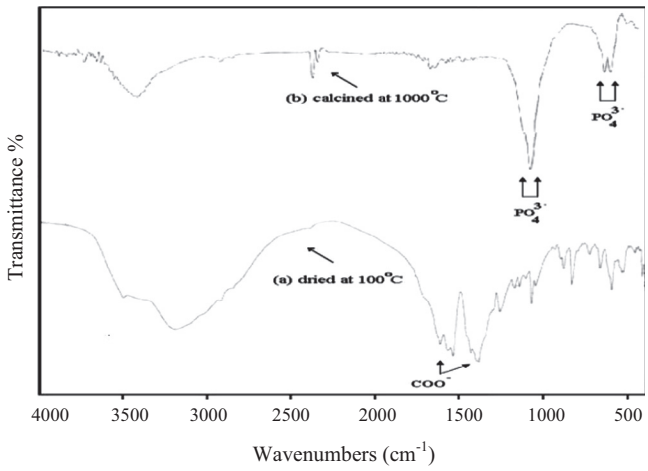

Fig. 2 IR spectra of the sample prepared (a) dried at 100 °C and (b) calcined at 1000 °C.

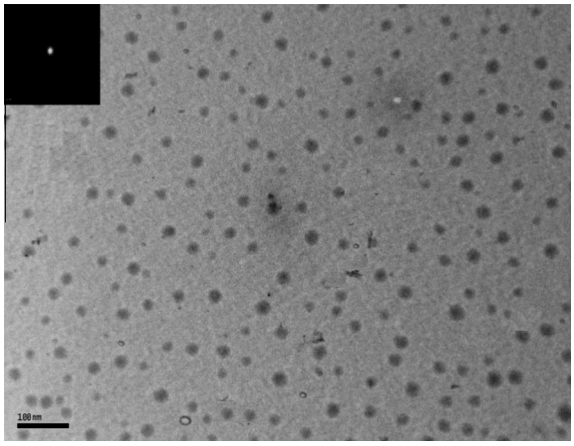

Fig. 4 TEM micrograph analysis of synthesized materials with its diffraction pattern.

phosphate particles to eliminate the implanted solid tumor in the thigh in addition to overcome the associated symptoms from affected skeletal muscle.

Material and methods

Particles preparation and characterization

A polymeric solution was prepared by dissolving 0.5 g of chitosan in 200 mL of 2% acetic acid while stirring for 24 h in 1-L flat round-bottomed flask. After complete dissolution of chitosan, a dissolved soluble calcium salt was added to polymeric media with stirring and heating until complete dissolution. Finally diammonium hydrogen orthophosphate was added to the mixture with natural Ca/P molar ratio while stirring and heating at 80 °C and completed to 500 mL with deionized water [12]. The final solution was filtrated and dried at 100 °C for 24 h then calcined at 1000 °C. The formed powder was characterized using The X-ray Diffraction (XRD), Fourier transform infrared (FTIR), Scanning electron microscopy (SEM), and Transmission electron microscope (TEM), which proved the synthesis of composite in nano range as shown in results.

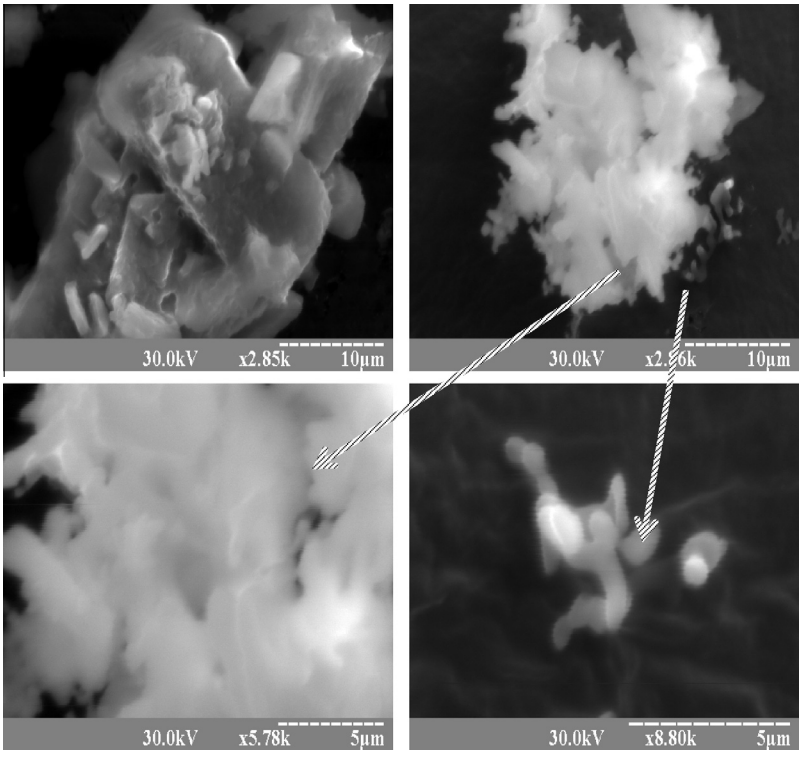

Fig. 3 SEM of calcined sample prepared at 1000 °C.

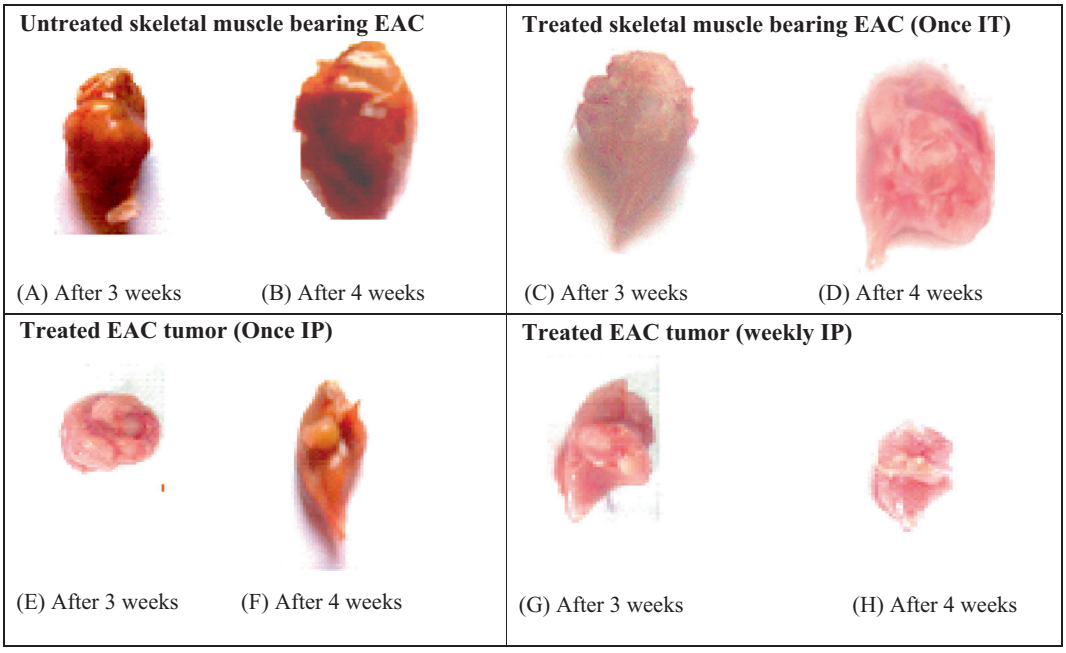

Fig. 5a Morphological features of EAC tumor in different groups.

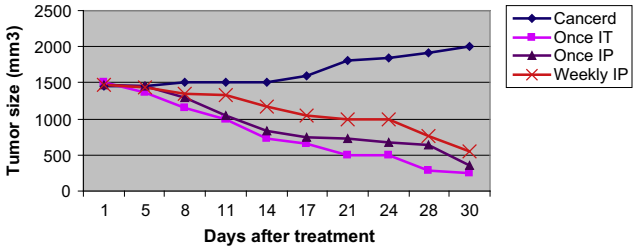

Fig. 5b EAC tumor size in different groups.

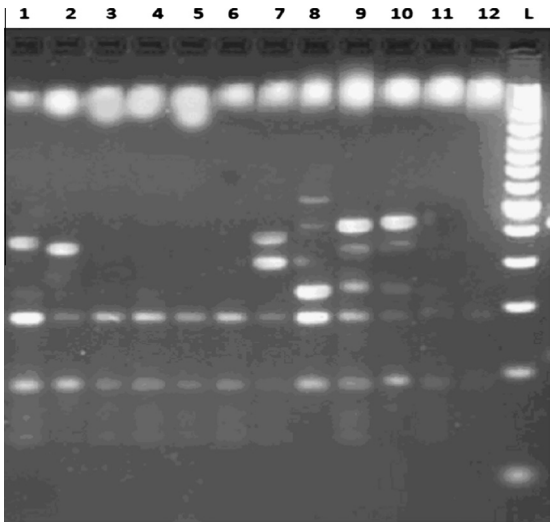

Fig. 6 DNA fragmentation of implanted tumor. Lanes (1 & 2): Once IT after 3 and 4 weeks respectively. Lanes (3 & 4): once IP nano-CaP after 3 weeks. Lanes (5 and 6): once IP nano-CaP after 4 weeks and (7 and 8) weekly IP nano-CaP after 3 weeks. Lanes 9 and 10 weekly IP nano-CaP after 4 weeks and 11 and 12 represent EAC without treatment.

Animals

85 Male Swiss albino mice weighing 20–22 g were used in the present study. They were acclimatized to the laboratory conditions prior to the study for seven days. The animals were kept at 25 ± 2 °C and a relative humidity of 40–45% with alternative day and night cycles of 12 h each. They were fed with pelleted rat chow and water *ad libitum*. *Anesthetic procedures and handling with animals were approved by and complied with the ethical guidelines of Medical Ethical Committee of the National Research Centre in Egypt (Approval number: 14077)*.

Tumor transplantation

Ehrlich Ascites Carcinoma (EAC) cells were chosen due to its high hematogenous metastatic propensity and reproducible biological behavior. EAC cells were collected by sterile disposable syringe from donor mice (Swiss albino) of 18–20 g body weight and suspended in sterile isotonic saline. The viability of the cells was 99% as judged by trypan blue exclusion assay. To asses a solid mass of Ehrlich tumor, a fixed number of viable cells 0.2 mL EAC cells containing 2×10^6 cells/mouse were inoculated intraperitoneally into the femoral region of recipient male mouse [13] and left for 7–10 days to allow tumor to grow as big as its diameter achieved 0.7–1.2 cm.

Treatment schedule

The animals were divided into nine groups: each equal 10 except group 9 comprises 5 animals. All groups received EAC cells (2×10^6 cells/mouse IP) and this day was considered

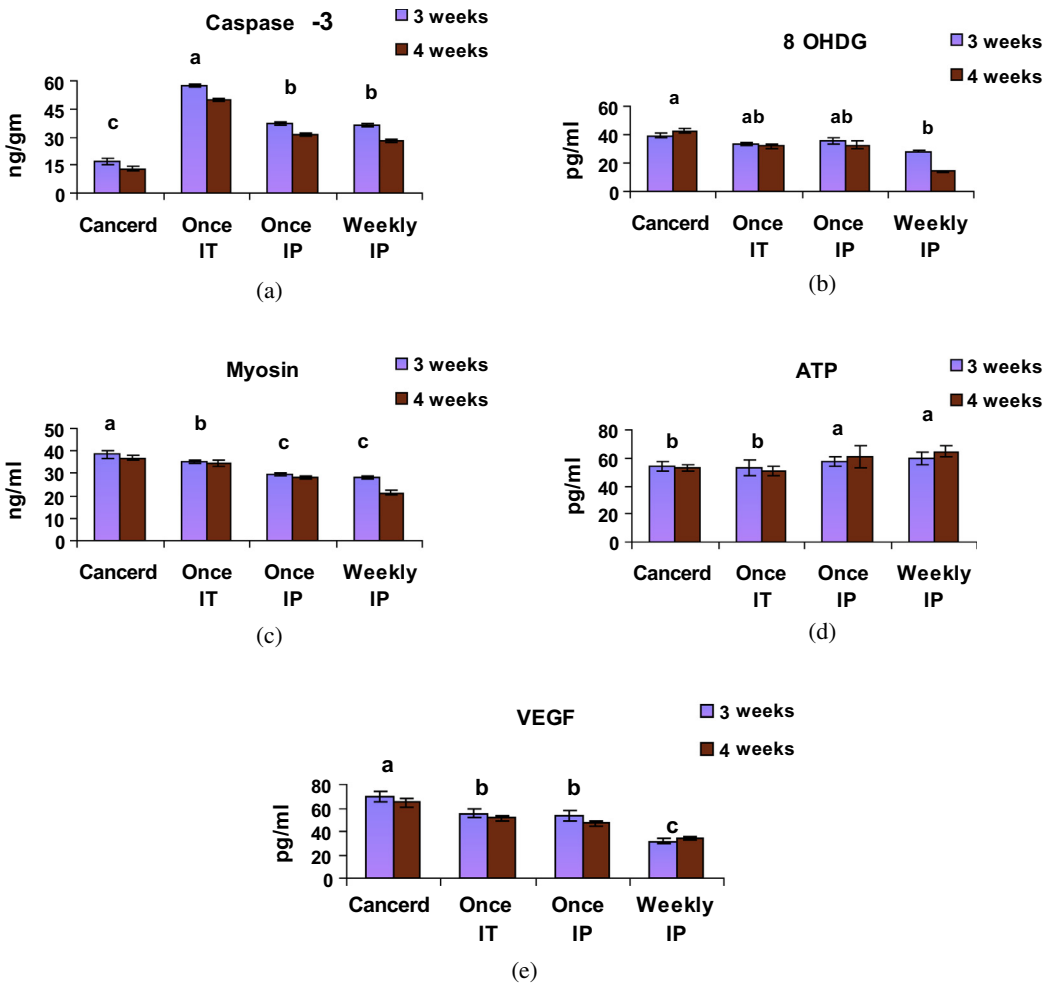

Fig. 7 (a) Serum caspase-3, b) OHDG, c) myosin, d) ATP, and e) VEGF levels in different groups.

as day zero. Groups 1 and 2 served as EAC control. Nine days after EAC transplantation, groups 3 and 4 were injected once intratumorally (IT) by nano-CaP (200 mg/kg body weight); groups 5 and 6 received nano-CaP once intraperitoneally (IP) and groups 7 and 8 received nano-CaP weekly (IP). Concerning the group 9, two animals were injected once and three animals were injected weekly for four weeks. The nano-CaP was thermally heated at < 1000 °C. The SEM analysis had shown fused grains with average size 70 nm. The ground fused grains were dispersed in sterile water before administration.

Tumor size

Tumor growth was monitored twice a week throughout the experimental work. The tumor growth was measured regularly using Vernier calipers and represented in terms of tumor size. The tumor size was estimated using the following formula: Tumor size (mm^3) = $4\pi(A/2)^2(B/2)$, where A is the minor tumor axis; B is the major tumor axis, and π equals to 3.14 [14]. The mean tumor size with the corresponding standard error was calculated in each experimental group.

Sample preparation

Blood samples and thigh skeletal muscle were collected after three weeks from groups 1, 3, 5, and 7 and after four weeks from groups 2, 4, 6, and 8. In case of group 9, the tissues were collected after 3 months to follow up the recurrence of tumor and to ensure the safety of muscle. Immediately Ehrlich tumor bearing thigh was excised and rinsed with saline. Small portion was placed in 10% phosphate-buffered formalin for histopathological examination. The rest was homogenized in 0.25 M ice-cold isotonic sucrose for DNA fragmentation and biochemical analyses.

DNA fragmentation

Qualitative analysis of DNA fragmentation was measured by agarose gel electrophoresis. Tumor cells were extracted from the animals and kept on ice during and after homogenization. Tissue samples were homogenized in chilled homogenization buffer (Ultra Turrax IKA T25-Germany) (pH 7.5), containing 75 mM NaCl and 24 mM Na2EDTA to obtain a 10% tissue solution, and then measured [15].

Biochemical analysis

Serum 8-hydroxy-deoxyguanosine (8-OHDG), myosin, and adenosine triphosphate (ATP) were assayed based on a solid phase enzyme linked immunosorbent assay (ELISA) (Life Sciences Advanced Technologies, Saint Petersburg FL 33710). Also, serum vascular endothelial growth factor (VEGF) (Boster Biological Technology LTD, Malden, MA, USA) and ELISA were determined according to the method of Ferrara [16]. Noradrenaline (NA) was measured using appropriate [^{125}I] radioimmunoassay kit (IBL, Hamburg, Germany) while dopamine (DA), serotonin, and gamma-aminobutyric acid (GABA) were estimated in the skeletal muscle [17].

Histopathological examination

Necropsy samples were collected from the skeletal muscle of mice thigh of different groups and fixed in 10% formol saline. Samples were washed with water and then serial dilutions of alcohols were used for dehydration. Specimens were cleared in xylene and embedded in paraffin at 56 °C in hot air oven. Paraffin bees wax tissue blocks were prepared for sectioning at 4 μm by sledge microtome. The obtained tissue sections were collected on glass slides, deparaffinized, stained by hematoxylin and eosin, and then examined through the electric light microscope [18].

Quantification of the percentage of tumor necrosis

Stained samples were subjected to reading and determination of necrosis areas, through the tumor mass using Auto CAD software (Free version for testing). After being scanned, the images were analyzed in AutoCAD software and areas of necrosis bounded by the electronic cursor were calculated in mm.

The following formula was used to calculate the percentage of necrosis:

$$\%\,\text{necrosis area} = (\text{necrosis area}/\text{total tumoral mass area}) \times 100$$

Statistical analysis

The data were statistically analyzed according to Steel and Torrie [19] using SPSS computer Program (v.17). The results were presented as mean ± SE. The differences between mean values were determined by two way analysis of variance (ANOVA) test, followed by Waller–Duncan k-ratio [20]. All statements of significance were based on probability of $P \leqslant 0.05$. Statistical significance of the relationships between variables was calculated by correlation analysis.

Results

Material characterizations

The X-ray Diffraction (XRD) analysis of the powder calcined at 1000 °C, identified the presence of different structures of calcium phosphate or tricalcium diphosphate Ca_3 $(PO_4)_2$ (these amounts were calculated using reference-intensity-ratio (RIR) method in XRD instrument semi-quantitatively) (Fig. 1) as the main characteristic bands of calcium phosphate

Table 1 The levels of serum caspase-3, 8OHDG, myosin, ATP and VEGF in cancer control and experimental groups.

Parameters	Groups											
	Cancer		Once IT		Once IP		Weekly IP		F1	F2		
	Time after treatment		Time after treatment		Time after treatment		Time after treatment					
	3 W	4 W	3 W	4 W	3 W	4 W	3 W	4 W				
Caspase-3 ng/g	$16.84^{b} \pm 1.49$	$13.0^{b} \pm 0.73$	$57.34^{a} \pm 0.84$	$50.11^{a} \pm 2.46$	$37.34^{a} \pm 1.59$	$31.30^{a} \pm 0.56$	$36.70^{a} \pm 1.68$	$28.11^{a} \pm 0.69$	58.05^{*}	$0.18^{\dagger}$		
8 OHDG Pg/mL	$39.30^{a} \pm 1.83$	$42.70^{a} \pm 1.67$	$33.50^{ab} \pm 1.27$	$31.98^{ab} \pm 1.49$	$35.60^{ab} \pm 1.74$	$32.50^{ab} \pm 2.81$	$28.10^{b} \pm 0.81$	$14.0^{b} \pm 0.66$	8.78^{*}	$1.84^{\dagger}$		
Myosin ng/mL	$38.55^{a} \pm 1.77$	$36.92^{a} \pm 1.35$	$35.32^{b} \pm 0.83$	$34.50^{b} \pm 1.15$	$29.31^{c} \pm 0.69$	$28.40^{c} \pm 0.72$	$28.11^{c} \pm 0.83$	$21.46^{c} \pm 1.32$	33.2^{*}	9.28^{*}		
ATP Pg/mL	$54.10^{b} \pm 3.08$	$52.90^{b} \pm 2.41$	$52.80^{b} \pm 5.26$	$50.8^{b} \pm 3.28$	$57.62^{a} \pm 3.02$	$60.91^{a} \pm 7.48$	$60.11^{a} \pm 4.48$	$64.60^{a} \pm 3.68$	10.29^{*}	$0.587^{\dagger}$		
VEGF Pg/mL	$69.90^{a} \pm 4.49$	$64.78^{a} \pm 3.84$	$55.42^{b} \pm 3.21$	$51.20^{b} \pm 2.59$	$53.81^{b} \pm 4.65$	$46.70^{b} \pm 2.69$	$31.73^{c} \pm 1.88$	$34.11^{c} \pm 0.98$	9.38^{*}	$0.89^{\dagger}$		

The different letters are statistically significant ($P < 0.05$). F1: different treatments (transplantation of solid tumor in mice and treatment with nano-CaP); F2: Time after treatment (weeks (W)).

* ($P < 0.05$).

† ($P > 0.05$).

at d = 2.87, 2.60, and 3.20 Å. While the Infrared analysis showed that the characteristic bands of PO_4^{3-} due to calcium phosphate structure ($Ca_3(PO_4)_2$) appeared clearly after calcinations (Fig. 2), the morphological analysis of the powder calcined at 1000 °C showed fused grains with crystal growth to form large crystals of a tubular shape and size from 0.5 to 10 µm. The large magnification clarified the molten grains of average grain size 500 nm (Fig. 3). Fig. 4 shows the TEM micrograph analysis of the synthesized calcium phosphates composite in nano range.

The EAC tumor of untreated mice grew faster than any other groups. The tumor not only rapidly shrunk in groups 5, 6, 7, and 8, but also they became nearly flat within 4 weeks post-treatment. Furthermore, in group 1 (untreated), central necrotic area was noted in the tumor that was enlarged till the 4th week (Figs. 5a and 5b).

DNA fragmentation of implanted tumor

DNA derived from animals bearing EAC, expressed distinct ladder pattern of DNA fragments (L) reaching less than 200 bp; a characteristic for apoptosis (lanes 1–10). The fragmentation pattern of nano-CaP treated cells was evident with various degrees depending on the way of injection and time. The DNA of untreated mice (EAC mice) was found to be intact as shown in lanes 11 and 12 (Fig. 6).

Biochemical findings

Fig. 7a–d represents the effect of CaP nanoparticles on some biochemical analysis in serum of different groups. Caspase-3 activity showed significant increase in all treated groups especially in mice groups injected intratumorally compared to untreated mice (Fig. 7a). A significant decrease in 8-OHdG, myosin, ATP, and VEGF levels was observed in experimental animals treated with nano-CaP compared to untreated animals (Fig. 7b–e). Additionally, the level of 8-OHDG was decreased after four weeks in mice injected weekly with nano-CaP (Table 1).

Statistical analysis showed significant increase in neurotransmitter levels (NA, DA, serotonin, and GABA) in skeletal muscle of nano-CaP treated groups compared to untreated group. The effect was more pronounced after four weeks in mice either injected only one time (once) or injected once a week as shown in Fig. 8a–d and Table 2.

Histopathological findings

Histopathological examination of the skeletal muscle under light microscope showed compact and aggregation of tumor cells within the muscular tissues in all wide implanted area. Ehrlich carcinoma showed groups of large, round, and polygonal cells, with pleomorphic shapes. The nuclei appeared hyperchromic and binucleated Fig. 9a–d.

According to histopathological results, treatment with nano-CaP diminished the majority of histopathological changes in the portal area after 3 weeks. Treatment of male mice bearing solid tumor by single dose of nano-CaP showed the presence of necrosis in 20% of implanted cancer cells after three weeks (Fig. 9e and f) and reached to 40% after four weeks (Fig. 9g and h).

Severe destruction and necrosis of tumor cells were recorded in solid tumor bearing mice treated weekly with nano-CaP. Necrosis was observed in 75% of the implanted cancer cells after three weeks (Fig. 9i) reaching to 80% after four weeks (Fig. 9j).

According to the histopathological results, necrosis was observed in 80% of the implanted cancer cells in mice bearing solid tumor and injected once intratumorally by nano-CaP after three weeks (Fig. 9k) and four weeks (Fig. 9l).

With respect to group 9, histopathological examination showed few inflammatory cells infiltration in focal manner at the muscle bundles (Fig. 9m), while the periphery zone showed focal inflammatory cells infiltration, red blood cells,

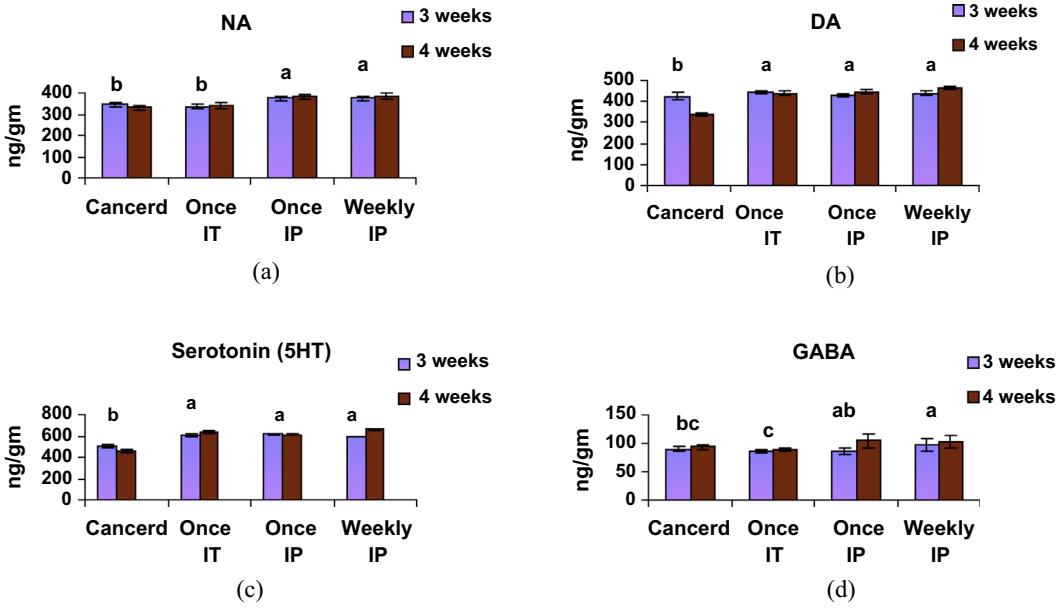

Fig. 8 (a) Tissue NA, b) DA, c) serotonin, and d) GABA levels in different groups.

Table 2 The levels of neurotransmitters (NA, DA, 5HT and GABA) in cancer control and experimental groups.

Parameters	Groups									
	Cancer		Once IT		Once IP		Weekly IP		F1	F2
	Time after treatment		Time after treatment		Time after treatment		Time after treatment			
	3 W	4 W	3 W	4 W	3 W	4 W	3 W	4 W		
NA ng/g	344.80^{b} ± 10.83	331.28^{b} ± 12.67	335.00^{b} ± 11.27	343.54^{b} ± 15.49	376.40a ± 9.74	381.50a ± 12.81	375.40a ± 10.81	382.90a ± 13.66	11.56*	0.027†
DA ng/g	425.80^{b} ± 15.77	338.90^{b} ± 7.35	443.50a ± 8.83	438.71a ± 10.15	430.90a ± 7.69	445.30a ± 11.72	438.20a ± 9.83	464.9a ± 5.32	7.00*	0.42†
5HT ng/g	503.25^{b} ± 9.08	458.00^{b} ± 11.41	606.30a ± 15.26	634.10a ± 11.28	615.50a ± 13.02	613.00a ± 7.38	593.50a ± 6.34	662.24a ± 8.68	4.192*	0.127†
GABA ng/g	90.12^{bc} ± 4.19	93.40^{bc} ± 3.81	85.90^{c} ± 3.29	89.30^{c} ± 2.59	86.11a^{b} ± 5.65	105.10a^{b} ± 12.67	98.30a ± 10.88	102.60a ± 12.18	7.27*	14.57*

The different letters are statistically significant ($P < 0.05$). F1: different treatments (transplantation of solid tumor in mice and treatment with nano-CaP); F2: Time after treatment (weeks (W)).
* ($P < 0.05$).
† ($P > 0.05$).

and edema in mice injected weekly (Fig. 9n and o). A nano-CaP injected once in solid tumor bearing mice achieved complete recovery of cancer cells, as edema was only detected between the muscle bundles as shown in (Fig. 9p).

Discussion

Ehrlich carcinoma, an undifferentiated carcinoma, is originally hyperdiploid, has high transplantable capability, no-regression, rapid proliferation, short life span, 100% malignancy and does not have tumor-specific transplantation antigen. It resembles human tumors, which are the most sensitive to chemotherapy. Following implantation of Ehrlich tumor cells, morphological and metabolic changes occur such as structural deterioration, decreased number of mitochondria, decreased DNA and RNA synthesis, loss of intracellular purine and pyrimidine nucleotides, nucleosides and bases and a decline of ATP concentration and turnover [14]. Nuclear morphology changes characteristic of apoptosis appear within the cell together with a distinctive biochemical event the endonuclease-mediated cleavage of nuclear DNA.

In the present study, nano-CaP inhibited the growth of tumor cells and induced morphological changes typical of apoptosis. The incidence of DNA fragmentation and increased level of caspase-3 of tumor cells confirmed such morphological findings. Treatment with nano-CaP induced ladder-like DNA fragmentation in tumor cells, which is a characteristic of DNA damage. Increased levels of DNA damage could cause the synthesis of a variety of incorrect proteins and therefore impaired cellular function [21]. Most anticancer drugs either natural or synthetic have been known to cause DNA damage or suppress its replication, not necessarily killing the cells directly but inducing apoptosis. During apoptosis, a specific nuclease (caspase-activated Dnase or CAD) cuts the genomic DNA between nucleosomes and generates apoptotic chromatin condensation and DNA fragments [21]. Among them, caspase-3 is a frequently activated death protease, catalyzing the specific cleavage of many key cellular proteins. Thus, caspase-3 is essential for certain processes associated with the dismantling of the cell and the formation of apoptotic bodies, but it may also function before or at the stage when commitment to loss of cell viability is made.

Skeletal muscle is the tissue with the largest mass in the body, and consists of post-mitotic cells, which are more prone to accumulate oxidative damage [22]. Thus, it is highly plausible that the muscle damage associated with muscle soreness causes oxidative damage by enhancement of free radical generation. The cytotoxic effects of free radicals include the oxidative damage of cellular DNA [23]. The inhibition of 8-OHdG level in serum of tumor bearing mice after nano-CaP treatment is strongly referable to the efficiency of material in scalable cancer cells and maintaining the integrity of DNA in the body cells. Adduct of 8-OHdG indicated oxidative DNA damage because this lesion is a frequently found adduct in mutated oncogenes and tumor suppressor genes [24]. Several tumor-derived vasoactive compounds have been pointed out to drive this increase in vascular permeability (VEGF) [25]. The thrust of nano-CaP regimen was to decrease VEGF level which is thought to be the single most important angiogenic cytokine in cancer and its secretion by tumor cells is responsible for initiation and maintenance of the ascites pattern of tumor growth [26]. It is well known that solid tumor growth requires the

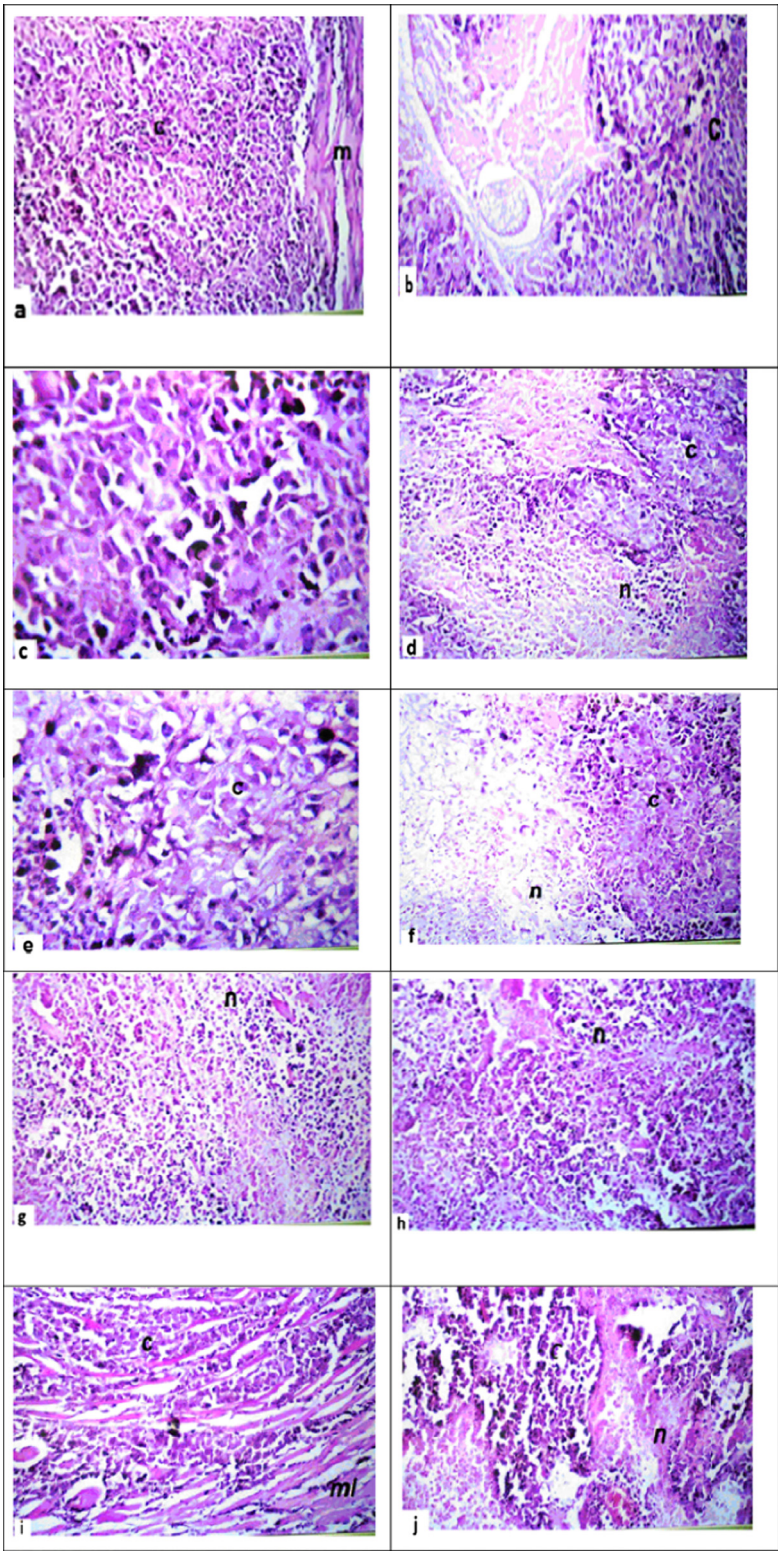

Fig. 9 (a–d) Skeletal muscle of mice bearing EAC, showed compact and aggregation of the tumor tissue cells spread within the muscular tissues. (e–h) Skeletal muscle of mice bearing EAC treated by single dose of nano-CaP after three weeks, showed the presence of necrosis in 20% of implanted cancer cells. (i) Skeletal muscle of solid tumor bearing mice treated weekly with nano-CaP after three weeks. (j) Skeletal muscle solid tumor bearing mice treated weekly with nano-CaP after four weeks. (k) Skeletal muscle of mice bearing solid tumor and injected once intratumorally by nano-CaP after three weeks. (l) Skeletal muscle of mice bearing EAC and injected once intratumorally by nano-CaP after four weeks. (m–o) Skeletal muscle of solid tumor bearing mice to follow-up of the treatment of nano-CaP after three months on cancer cells invasion in thigh skeletal muscle, and p-once injection of nano-CaP in solid tumor bearing mice achieved complete recovery of cancer cells after three months.

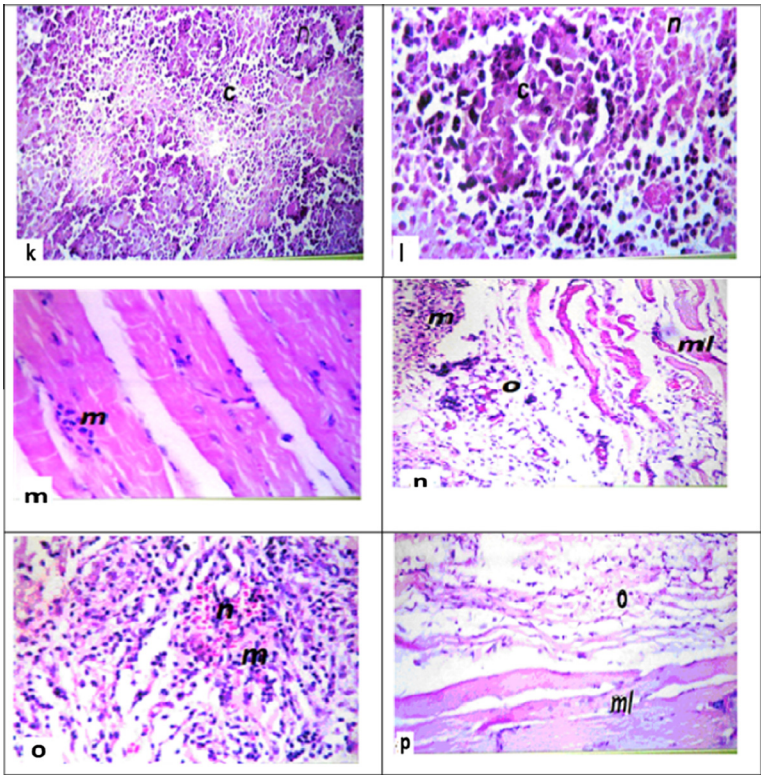

Fig 9. *(continued)*

generation of new blood vessels from an established vascular network. The newly formed vascular network provides necessary nutrients and oxygen to meet the increased metabolic demand of the growing tumor and increase the probability of tumor dissemination via the vascular system [27]. Interestingly, tumor tissues lack a lymphatic system for eliminating lipophilic and polymeric materials from them; therefore, once the particles penetrate the tumor tissues, they cannot be eliminated easily. Thus, tumors exhibit enhanced penetration and retention effect for 50- to 100-nm particles [28]. Long-circulating nanoparticles with the appropriate particle size have more frequent opportunities to encounter 'leaky tumor capillaries' and extravasate into the tumor tissue [29]. On the other hand, accompanying between levels of myosin with ATP in tumor bearing mice is consistent with biological rationality. Since, myosin is released into the circulation following muscle injury and acts as an ATPase. It can hydrolyze ATP to generate the force for the contraction of muscle cells and movement along actin filaments necessary to drive a wide variety of cellular functions [30].

The most important rendering of nano-CaP therapy observed in the present study was improvement of neurotransmitters content in thigh muscle because novel neurological aspects of tumors were more elucidated and many evidences have further shown that tumors growth process is also related to the nervous system. More important, numerous neurotransmitters influence tumor vascularization and cell migration [31]; in addition, they may also suppress the immune response in cancer [32]. These influences are increased by the ability of the cancer cells to secret neurogenic factors [33], which influences neurons development. Numerous papers have pointed a correlation between the GABA and tumor cells migration, indicating a local antitumor effect of GABA [34]. Another neurotransmitter, which is the dopamine, plays an important role within the neuro-tumoral interactions and has effects on both cancer growth and anticancer drugs. It blocks VEGF-induced angiogenesis of endothelial progenitors in the bone marrow and contributes in the growth diminution of cancers. In this aspect, further evidence provided by [35,36] that DA can inhibit the functions of adult endothelial cells by suppressing phosphorylation of vascular endothelial growth factor receptor 2 (VEGFR2), focal adhesion kinase (FAK), and mitogen-activated protein kinase (MAPK) and by acting through its D2 receptors, can inhibit the mobilization of BM-derived endothelial progenitor cells (EPCs). Joseph et al. [37] reported that GABA could inhibit colon cancer migration associated with the norepinephrine-induced pathway [38]. On the other hand, Alves et al. [39] reported a decrease in hypothalamic noradrenaline (NA) levels and increase in NA turnover in Ehrlich tumor-bearing mice.

The performance of CaP nano-particles validated the general view of the literature because the development of multifunctional nanoparticles might eventually render nanoparticles able to target and kill cancer cells simultaneously providing low side effects [40]. Targeting tumor tissues occurs through the extravasations of nanoparticles post-injection into the systemic blood circulation. The biodistribution of these particles is dependent on the characteristics of blood capillaries in the organs and tissues as well as the administration site, particle size and particle surface properties. Even in intratumoral (IT) administration, understanding the mechanism of the extravasations is critical to retain the particles at the injection sites. In addition to such macro bio-distribution of particles, their diffusion in the tissues, association to cells,

internalization into the cells and intracellular distribution are important issues in cancer therapy and diagnosis [41].

Owing to general histopathological observations agreed to potency of nano-CaP in DNA fragmentation of tumor cells included a great percentage of necrotic tumor cells increase with time. Interestingly, the extension of pathological examination to three months reflects the irreversible mode of nano-CaP therapy. The specimen of skeletal muscle appeared devoid of any tumor cells but contained only few inflammatory cells and edema.

Conclusions

The newly-formed nano-calcium phosphates particle had shown good biocompatibility and low cytotoxicity to normal cells when injected intraperitoneally. It has potent therapeutic effect on implanted solid tumor within four weeks and achieved complete recovery of EAC after three months. This study provides a comprehensive insight into the mode of action of the usage of nanoparticle of CaP *in vivo* as a therapy of solid tumor.

Conflict of interests

The authors have declared no conflict of interest.

Acknowledgments

The authors are grateful to Dr. Adel M. Bakeer Kholoussy, Department of Pathology, Faculty of Veterinary Medicine, Cairo University for his helping in the examination of the histopathological slides and for his valuable comments.

References

[1] Grobmyer SR, Morse D, Fletcher B. The promise of nanotechnology for solving clinical problems in breast cancer. J Surg Oncol 2011;103(4):317–25.
[2] Bhaskar S, Furong T, Stoeger T. Multifunctional Nanocarriers for diagnostics, drug delivery and targeted treatment across blood–brain barrier: perspectives on tracking and neuroimaging. Particle Fibre Toxicol 2010;7:3.
[3] Singhal S, Nie S, Wang MD. Nanotechnology applications in surgical oncology. Annu Rev Med 2010;61:359–73.
[4] Sakhrani NM, Padh H. Organelle targeting: third level of drug targeting. Drug Des Devel Ther 2013;7:585–99.
[5] Reichert JM, Wenger JB. Development trends for new cancer therapeutics and vaccines. Drug Discov 2008;13:30–7.
[6] Fu G, Vary PS, Lin CT. Anatase TiO_2 nanocomposites for antimicrobial coating. J Phys Chem 2005;109:8889–98.
[7] Hong RY, Liu R, Feng B, Li HZ. Double miniemulsion preparation for hybrid latexes. In: Miniemulsion polymerization: recent advances; 2010. p. 251–75 [Chapter 9].
[8] Goldberg M, Langer R, Jia X. Nanostructured materials for applications in drug delivery and tissue engineering. J Biomater Sci Polym 2007;18(3):241–68.
[9] Fukumori Y, Ichikawa H. Nanoparticles for cancer therapy and diagnosis. Adv Powder Technol 2006;17(1):1–28.
[10] Sahdev P, Podaralla S, Kaushik RS, Perumal O. Calcium phosphate nanoparticles for transcutaneous vaccine delivery. J Biomed Nanotechnol 2013;9(1):132–41.
[11] Haedicke K, Kozlova D, Gräfe S, Teichgräber U, Epple M, Hilger I. Multifunctional calcium phosphate nanoparticles for combining near-infrared fluorescence imaging and photodynamic therapy. Acta Biomater 2015;14:197–207.
[12] Yamanguchi S, Lizuka A, Monma OH, Tanaka J. The effect of citric acid addition on chitosan/hydroxyapatite composites. Colloids Surf A 2003;214:111–8.
[13] Gothoskar SV, Ranadive KJ. Anticancer screening of SAN-AB: an extract of marking nut Semicarpus anacardium. Indian J Exp Biol 1971;9:372–5.
[14] Abdel-Rahman MN, Kabel AM. Comparative study between the effect of methotrexate and valproic acid on solid Ehrlich tumour. J Egyptian Natl Cancer Inst 2012;24:161–7.
[15] loannou YA, Chen FW. Quantitation of DNA fragmentation in apoptosis. Nucl Acids Res 1996;24(5):992–3.
[16] Ferrara N. VEGF. In: Oppenheim JJ, Feldman M, editors. Cytokine reference volume 1: ligands. London, UK: Academic Press; 2001. p. 791–803.
[17] Zagrodzka J, Romaniuk A, Wieczorek M, Boguszewski P. Bicuculline administration into ventromedial hypothalamus: effects on fear and regional brain monoamines and GABA concentrations in rats. Acta Neurobiol Exp 2000;60(3):333–43.
[18] Banchroft JD, Stevens A, Turner DR. Theory and practice of histological techniques. 4th ed. Churchil Livingstone, New York, London, San Francisco, Tokyo; 1996.
[19] Steel RGD, Torrie JH. Principles and procedures of statistics. NewYork: McGraw-Hill; 1980.
[20] Waller RA, Duncan DB. A Bayes rule for the symmetric multiple comparisons problem. J Am Stat Assoc 1969;64:1484–503.
[21] Lawal RA, Ozaslan MD, Odesanmi OS, Karagoz ID, Kilic IH, Ebuehi OA. Cytotoxic and antiproliferative activity of Securidaca longepedunculata aqueous extract on Ehrlich ascites carcinoma cells in Swiss albino mice. Int J Appl Res Natural Prod 2013;5(4):19–27.
[22] Zsolt AK, Pucsok J, Mecseki S. Soreness-induced reduction in force generation is accompanied by increased nitric oxide content and DNA damage in human skeletal muscle. Free Radical Biol Med 1999;26(7/8):1059–63.
[23] Zsolt K, Naito H, Kaneko T. Exercise training decreases DNA damage and increases DNA repair and resistance against oxidative stress of proteins in aged rat skeletal muscle. Pflugers Arch Eur J Physiol 2002;445:273–8.
[24] Valko M, Rhodes CJ, Moncol J. Free radicals, metals and antioxidants in oxidative stress-induced cancer. Chem Biol Interact 2006;160:1–4.
[25] García-Román J, Zentella-Dehesa A. Vascular permeability changes involved in tumor metastasis. Cancer Lett 2013;335(2):259–69.
[26] Ghosh S, Roy M, Banerjee P, Maity J. Modulation of tumor induced angiogenesis in Ehrlich ascites tumor. Exp Clin Cancer Res 2004;23:4.
[27] Isenberg JS, Hyodo F, Ridnour LA. Thrombospondin 1 and vasoactive agents indirectly alter tumor blood flow. Neoplasia 2008;10(8):886–96.
[28] Qi X, Maitani Y, Nagai T, Wei S. Comparative pharmacokinetics and antitumor efficacy of doxorubicin encapsulated in soybean-derived sterols and poly(ethylene glycol) liposomes in mice. Int J Pharm 1997;146(1):31–9.
[29] Sellers James R. Myosins: a diverse superfamily. Biochim Biophys Acta 2000;1496(1):3–22.
[30] Lang K, Drell T, Lindecke A. Induction of a metastatogenic tumor cell type by 419 neurotransmitters and its pharmacological inhibition by established drugs. Int J Cancer 2004;112:231–8.
[31] Godbout JP, Glaser R. Stress-induced immune dysregulation: implications for wound healing, infectious disease and cancer. J Neuroimmune Pharmacol 2006;1:421–7.

[32] Dolle L, El Yazidi-Belkoura I, Adriaenssens E. Nerve growth factor overexpression and autocrine loop in breast cancer cells. Oncogene 2003;22:5592–601.
[33] Ghanemi A. Tumors, Neurotransmitters and Pharmacology: Interactions and Implications. Int J Public Health Sci (IJPHS) 2013;2(1):17–22.
[34] Ferrara N, Kerbel RS. Angiogenesis as a therapeutic target. Nature 2005;438:967–74.
[35] Chakroborty D, Chowdhury UR, Sarkar C, Baral R, Dasgupta PS, Basu S. Dopamine regulates endothelial progenitor cell mobilization from mouse bone marrow in tumor vascularization. J Clin Invest 2008;118(4):1380–9.
[36] Spiegel A, Shivtiel S, Kalinksovich A, Ludin A, Netzer N, Goichberg P. Catecholaminergic neurotransmitters regulate migration and repopulation of immature human CD34+ cells through Wnt signaling. Nat Immunol 2007;8:1123–231.
[37] Joseph J, Niggemann B, Zaenker KS, Entschladen F. The neurotransmitter gamma-aminobutyric acid is an inhibitory regulator for the migration of SW 480 colon carcinoma cells. Cancer Res 2001;62:6467–9.
[38] Hui YL, Liu Y, Dong YL, Liu YH, Li F, Ju Q, et al. GABA stimulates human hepatocellular carcinoma growth through overexpressed GABAA receptor theta subunit. World J Gastroenterol 2012;18(21):2704–11.
[39] Alves GJ, Vismari L, Lazzarini R, Merusse JL, Palermo-Neto J. Odor cues from tumor-bearing mice induces neuroimmune changes. Behav Brain Res 2012;214(2):357–64.
[40] Mora F, Segovia G, Del Arco A, de Blas M. Stress, neurotransmitters, corticosterone and body-brain integration. Brain Res 2012;1476:71.
[41] Hernández-Pedro NY, López ER, Maldonado RM, Cruz VP, Abel Santamaría A, Pineda B, et al. Application of nanoparticles on diagnosis and therapy in gliomas. Biomed Res Int 2013;2013:351031.